Picosecond Time-Resolved Absorption Studies of the Solvation of $Cr(CO)_5$ in Alcohols: A Unimolecular Kinetic Model for the Formation of $Cr(CO)_5(OHR)$ from Photogenerated $Cr(CO)_5(ROH)$

Xiaoliang Xie and John D. Simon*,†

Contribution from the Department of Chemistry, B-041, University of California at San Diego, La Jolla, California 92093. *Received June 21, 1989*

Abstract: Picosecond absorption spectroscopy is used to examine the photodissociation of $Cr(CO)_6$ in alcohol solutions. In the series of linear alcohols (n = 1-8), photodissociative loss of CO occurs within the time resolution of the experiment, indicating dissociation in <0.5 ps. The time-resolved spectra clearly show that immediately following photolysis, the primary intermediates formed are a distribution of solvated complexes involving coordination of either an alkane or a hydroxyl group of the solvent to the photogenerated coordination site on the metal. The spectral evolution reveals that the alkane-coordinated complexes undergo rearrangement to form the more stable hydroxyl-coordinated species. The dynamics of this rearrangement process are found to be inconsistent with a dissociative mechanism. Comparison of the time-dependent populations of the alkane and hydroxyl complexes in ethanol, 1-propanol, and 2-propanol suggests that the change in coordination occurs by a unimolecular process, not a bimolecular displacement reaction. A kinetic model for a unimolecular rearrangement mechanism is proposed and compared to the experimental data. The kinetic model allows for the examination of the effect of different distributions of initially formed complexes on the reaction rates. In particular, initial coordination occurring randomly along the solvent chain or a preferential bonding to a terminal site of the solvent is addressed in detail. Comparison between the simulated and experimental data supports the conclusion that the initial coordination of the solvent molecule to the $Cr(CO)_5$ fragment occurs randomly.

The photochemistry of $Cr(CO)_6$ in solution has been the subject of many recent experimental and theoretical studies.[1-6] In the past few years, several picosecond time-resolved studies have been reported.[1-4] These studies have focused on the time scale of the dissociation and the subsequent dynamics of the photogenerated $Cr(CO)_5$ fragment. Optical studies of $Cr(CO)_5L$ complexes in neat solutions and rare-gas matrices[7] show that the absorption spectrum is sensitive to the solvent (or matrix) ligand, L. Absorption spectra with a maximum from 620 nm (L = (perfluoromethyl)cyclohexane solution (PFMCH), neon matrix) to 300 nm (L = CO) have been reported. The magnitude of the blue shift, compared to Ne or PFMCH, is commonly attributed to increased bonding interactions between the chromium metal and the ligand. Time-resolved studies indicate that once these complexes are formed, even for weakly interacting ligands, i.e., PFMCH, the hexacoordinate species are stable for many nanoseconds.

Despite the large number of studies on the photodissociation of $Cr(CO)_6$ in solution, the exact mechanism and states involved in the photodissociative process and the subsequent solvation of $Cr(CO)_5$ have not unambiguously been determined. Theoretical calculations by Hay[6] indicate that photodissociation of CO from the first excited state creates an electronically excited $Cr(CO)_5$ fragment with C_{4v} symmetry. This species relaxes to the ground state by interconverting between C_{4v} and D_{3h} isomers, randomizing the location of the vacant coordination site on the metal. Matrix photolysis studies on $Cr(CO)_6$ using polarized light reveal that the $Cr(CO)_5$ fragment can isomerize via a square pyramid → trigonal bipyramid → square pyramid mechanism.[7c] Under the assumption that those molecules which do not result in "moving" the vacant coordination site undergo geminate recombination with the photoeliminated CO, the maximum quantum yield for dissociation predicted by this isomerization mechanism is 0.67,[8] in excellent agreement with quantum yields reported for various substitution reactions. Recent femtosecond results find that bond breakage occurs in <0.25 ps.[2] Following dissociation, rapid coordination of a solvent molecule, L, to the site vacated by the photoeliminated CO is observed. Evidence for excited-state $Cr(CO)_5$ is also presented.

In recent reports, we have demonstrated that the dynamics of solvation of the $Cr(CO)_5$ fragment can be followed by monitoring the time dependence of the optical spectrum of the chromium complex.[1] Examining the photolysis of $Cr(CO)_6$ in methanol, we found that the absorption band characteristic of the $Cr(CO)_5$-(MeOH) complex revealed a 2.5-ps rise time.[1a] This observation was near the limits of our time resolution but has recently been confirmed by Nelson and co-workers using <100-fs laser pulses.[2] These results were interpreted in terms of the solvent restructuring needed for the formation of the Cr-L bond. For the photolysis of $Cr(CO)_6$ in long-chain alcohol solutions, solvent coordination to the $Cr(CO)_5$ fragment resulted in the initial formation of both alkane, $Cr(CO)_5(ROH)$, and hydroxyl, $Cr(CO)_5(OHR)$, complexes.[1b] With increasing delay time, the alkane complexes were observed to thermally rearrange to the more stable hydroxyl species. The dynamics of this rearrangement process could be followed by examining the time dependence of the transient absorption of the $Cr(CO)_5(HOR)$ and $Cr(CO)_5(ROH)$ absorption bands, probed at 460 and 520 nm, respectively. Several mechanisms for the rearrangement process can be envisioned. These

† NSF Presidential Young Investigator (1985-1990) and Alfred P. Sloan Fellow (1988-1990).

(1) (a) Simon, J. D.; Xie, X. *J. Phys. Chem.* **1986**, *90*, 6751. (b) Simon, J. D.; Xie, X. *J. Phys. Chem.* **1987**, *91*, 5538. (c) Simon, J. D.; Xie, X. *J. Phys. Chem.* **1989**, *93*, 291. (d) Xie, X.; Simon, J. D. *J. Phys. Chem.* **1989**, *93*, 4401.

(2) Joly, A. G.; Nelson, K. A. *J. Phys. Chem.* **1989**, *93*, 2876.

(3) (a) Yang, G. K.; Peters, K. S.; Vaida, V. *Chem. Phys. Lett.* **1986**, *125*, 566. (b) Bernstein, M.; Simon, J. D.; Peters, K. S. *Chem. Phys. Lett.* **1983**, *100*, 241. (c) Simon, J. D.; Peters, K. S. *Chem. Phys. Lett.* **1983**, *98*, 53.

(4) (a) Wang, L.; Zhu, X.; Spears, K. G. *J. Am. Chem. Soc.* **1988**, *110*, 8695. (b) Wang, L.; Zhu, X.; Spears, K. G. *J. Phys. Chem.* **1989**, *93*, 2.

(5) (a) Kelley, J. M.; Bent, D. V.; Hermann, H.; Schulte-Frohlinde, D.; Van Gustorf, E. K. *J. Organomet. Chem.* **1974**, *69*, 259. (b) Bonneau, R.; Kelley, J. M. *J. Am. Chem. Soc.* **1980**, *102*, 1220. (c) Kelley, J. M.; Long, C.; Bonneau, R. *J. Phys. Chem.* **1983**, *87*, 3344.

(6) Hay, P. J. *J. Am. Chem. Soc.* **1978**, *100*, 2411.

(7) (a) Perutz, P. N.; Turner, J. J. *J. Am. Chem. Soc.* **1975**, *97*, 4791. (b) Perutz, R. N.; Turner, J. J. *Inorg. Chem.* **1975**, *14*, 262. (c) Burdett, J. K.; Gzybozwki, J. M.; Perutz, R. N.; Poliakoff, M.; Turner, J. J.; Turner, R. F. *Inorg. Chem.* **1978**, *17*, 146. (d) Turner, J. J.; Burdett, J. K.; Perutz, R. N.; Poliakoff, M. *Pure Appl. Chem.* **1977**, *49*, 271. (e) Burdett, J. K. *Coord. Chem. Rev.* **1978**, *27*, 1. (f) Burdett, J. K.; Graham, M. A.; Perutz, R. N.; Poliakoff, M.; Rest, A. J.; Turner, J. J.; Turner, R. F. *J. Am. Chem. Soc.* **1975**, *97*, 4805.

(8) (a) Nasielski, J.; Colas, A. *Inorg. Chem.* **1978**, *17*, 237. (b) Nasielski, J.; Colas, A. *J. Organomet. Chem.* **1975**, *101*, 215.

0002-7863/90/1512-1130$02.50/0

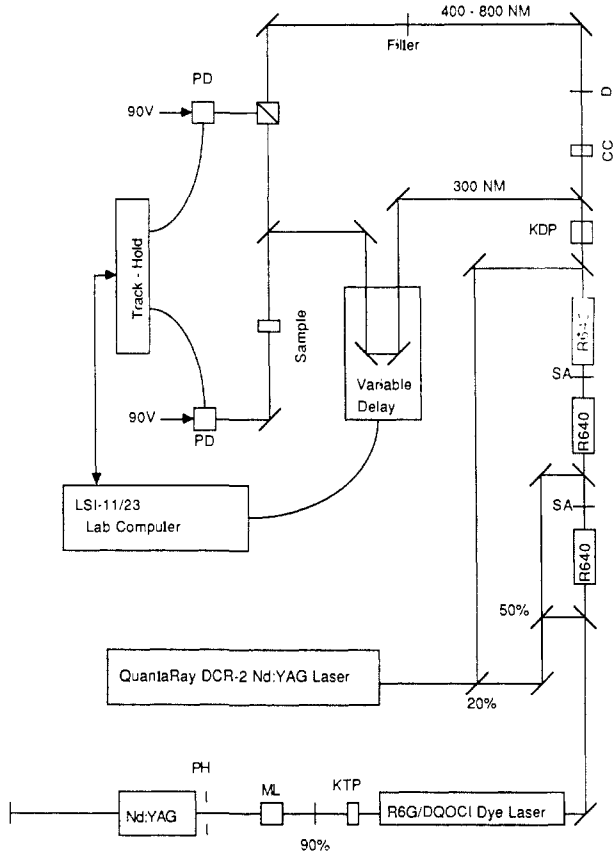

Figure 1. Block diagram of the picosecond absorption spectrometer. The following abbrevations are used: PH, pin hole; ML, acoustooptic mode locker; SA, saturable absorber jet (crystal violet in ethylene glycol); R640, Rhodamine-640 dye cell; PD, DT-110 photodiode; CC, continuum cell; D, diffuser.

include solvent exchange by a dissociation mechanism (or dissociation followed by rotation and recoordination of a single solvent molecule), an associative substitution reaction, and solvent migration via a unimolecular rearrangement process. In an initial study examining the dynamics in 1-propanol (1-Pro) and 2-propanol (2-Pro), the rate of restructuring was found to occur faster in 2-Pro than in 1-Pro.[1c] Comparison with known bond strengths for the Cr–alkane bond and the observation that the dynamics in 2-Pro was similar to that found in ethanol suggested that the restructuring of these primary complexes is occurring by a unimolecular mechanism.

In the present paper, the rearrangement process $Cr(CO)_5(ROH) \rightarrow Cr(CO)_5(HOR)$ is examined in detail. In particular, by comparison of the dynamics observed in neat alkane solvents and the series of alcohols, insight into the rearrangement mechanism can be obtained. Various mechanisms are examined. We find that both a dissociative mechanism and an associative substitution mechanism are inconsistent with the experimental results. A unimolecular reaction mechanism is proposed. The model allows for the examination of the effect of different initial distributions of initially formed solvent complexes on the reaction rates. Two limiting cases are examined in detail: random coordination along the solvent chain and preferential bonding to the terminal sites of the solvent. The experimental data are compared to simulated time-dependent absorption data using these models. The model has only one undetermined parameter, the rate constant for migration between neighboring carbons, k_{C-C}. We find that the data for propanol through octanol can be accurately modeled by the random coordination model using a single rate for k_{C-C}.

Experimental Section

A block diagram of the experimental apparatus is shown in Figure 1. A CW Nd^{3+}:YAG laser (Quantronix Model 116) is actively mode locked at 38 MHz. The output (9 W) is doubled by focusing the IR light with a 10-cm lens into a 0.8-cm KTP crystal, resulting in the generation of 1.5 W at 532 nm. This light is used to synchronously pump a Rhodamine-6G/DQOCl dye laser (Coherent 702-1). At 600 nm, an output power of 100 mW is obtained. The addition of the saturable absorber, DQOCI, eliminates the side wings of the pulse and results in substantial shortening of the pulse.[9] Autocorrelation measurement using a noncollinear geometry (InRad 5-14) indicates a pulse width of approximately 0.7 ps (FWHM).

The dye laser output is amplified with a three-stage longitudinally pumped pulsed dye amplifier.[10] The amplifier is driven by a nanosecond Nd^{3+}:YAG laser (QuantaRay DCR-2(20)), providing 130 mJ at 532 nm at a repetition rate of 20 Hz. The three cells are pumped by 15, 15, and 100 mJ of green light, respectively. The beam diameters in the three cells are 2, 2, and 7 mm, respectively. Rhodamine-640 in methanol is used as the amplifying medium. Saturable absorber jets of crystal violet in ethylene glycol are used to isolate the stages of the amplifier. The amplified laser pulse are 0.8 ps (FWHM) and 1-2 mJ/pulse, ±10 (percent pulse–pulse fluctuation), with a pulse energy to amplified spontaneous emission (ASE) ratio better than 100:1. Without the saturable absorber jets isolating the three stages, the ASE energy is approximately 3 times the pulse energy.

The output of the amplifier is telescoped to a beam diameter of 2 mm and then frequency doubled by a 0.2-cm angle-tuned KDP crystal (Quantum Technologies). The resulting 300-nm UV light, ≈100 μJ, serves as the photolysis beam. It is separated from the 600-nm light with a dichroic beam splitter, passed down a computer-controlled optical delay line (Velmex, resolution of 40 fs/step), and focused on the sample with a 20-cm planoconvex quartz lens. The remaining 600-nm radiation is focused into a 5-cm cell of water, generating a white light continuum. The picosecond continuum light extends from 400 to 800 nm and is used to record the transient absorption data.

Reaction dynamics are monitored by measuring the time dependence of the absorbance of transient intermediates at a fixed wavelength in the continuum. Interference filters (ESCO, FWHM ≈ 5 nm) are used to select the desired probe wavelength. With narrow-band interference filters, the group velocity dispersion associated with the probe continuum is negligible. In order to eliminate the spatial hopping of the continuum beam, the white light is focused on a diffuser; the scattered light is collected through a 0.25-in. aperture and collimated with a 20-cm planoconvex lens immediately after the aperture. This homogeneous beam is split into two beams of equal intensity. One beam serves as a reference beam, I_0; the other serves as the probe beam, I, and is focused collinearly with the pump beam through the sample. After the sample, a glass filter, transparent to the visible probe light, is used to block any UV photons that are not absorbed by the sample. Both the reference and probe beams are detected by large-area photodiodes (E.G.G. DT-110). The diode output is integrated with a sample-and-hold circuit (Stanford Research System, Model 248). Neutral-density filters are used to ensure that the intensities of the two beams are in the linear response region of the photodiodes. The output of the sample-and-hold circuit is digitized by a laboratory computer (LSI-11/23$^+$). A computer-controlled shutter in the UV beam enables the measurement of the absorbance with and without the UV excitation. The transient absorbance signal is then calculated by using the following expression:

$$\Delta A(t) = \log (I_0(t)/I(t))_{\text{with excitation}} - \log (I_0(t)/I(t))_{\text{without excitation}} \quad (1)$$

In general, 200 laser shots are averaged for each transient absorbance value. Under these conditions, signals as small as $\Delta A \approx 0.001$ are easily detected. A total decay scan of 2 ns, collecting the transient absorption in 10-ps steps, requires 30 min to complete.

Before and after each experiment, the alignment of the delay line is checked by measuring the transient absorption of benzophenone. Upon excitation benzophenone undergoes intersystem crossing in a few picoseconds and thus should have a constant triplet–triplet absorption for tens of nanoseconds. The instrument response is determined by measuring the rise of the $S_1 \rightarrow S_N$ absorption of *trans*-stilbene. These measurements were consistent with autocorrelation measurements of the laser pulse.

When the pump and probe beams were coincident in time, we observed a small background signal in a sample of pure solvent. This is in agreement with the observations of many other groups; however, we are not certain of the origin of this signal. The amplitude of this signal, <0.01 OD, is negligible in comparison to the absorbance observed for the chromium complexes probed in the region from 420 to 550 nm. However, this effect makes measurements of dynamics processes on the order of our laser pulse unreliable. In addition, we attempted to record transient absorption kinetics in the wavelength range from 600 to 700 nm. Unfortunately, at these wavelengths, the short-lived (1–10 ps) transient signals observed in pure solvent samples were comparable to that found

(9) Mourou, G. A.; Sizer, T., III. *Opt. Commun.* **1982**, *41*, 47.
(10) See, for example: Koch, T. L.; Chiu, L. C.; Yariv, A. *Opt. Commun.* **1982**, *40*, 364.

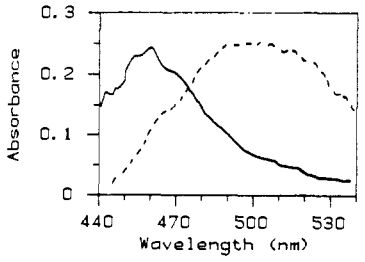

Figure 2. Time-resolved absorption spectra of $Cr(CO)_5$ recorded 50 ps after the photolysis of $Cr(CO)_6$ in cyclohexane (---) and in methanol (—). The maximum absorbance for each complex is at 505, and 460 nm, respectively.

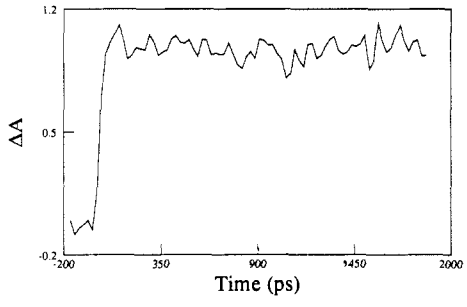

Figure 3. Time-resolved absorption kinetics at 520 nm for the photolysis of $Cr(CO)_6$ in cyclohexane. These data show an instantaneous rise in the transient signal with no change in absorbance for several nanoseconds.

for chromium solutions. Thus, we are not able to quantitatively determine whether or not the primary products of photolysis absorb in this wavelength region.

$Cr(CO)_6$ was purchased from Aldrich and purified by sublimation. Cyclohexane and the alcohols were all spectral grade. All solvents were dried over 3A molecular sieves. The samples were prepared in the dark and purged with dry N_2. The concentration of metal carbonyl, about 10^{-3} M (saturated), ensured that almost all of the UV excitation light (>95%) was absorbed in a 1-cm sample cell. In order to prevent the buildup of photoproducts, a flowing sample was used. Approximately 500 mL of $Cr(CO)_6$ solution was used for each experiment. The flow rate was such that new sample was in the focal volume for each laser shot. Polarization effects on the time dependence of the transient absorption signals were examined by collecting data using parallel, perpendicular, and magic angle polarized light with respect to the excitation beam. No polarization effects were observed.

Data analysis and kinetic calculations were performed on a Sun 3/110 computer system.

Results

In Figure 2, transient absorption spectra obtained 50 ps after photolysis of $Cr(CO)_6$ in cyclohexane and in methanol are shown. For these two solvents, the solvated complex has an absorption maximum at 505 and 460 nm, respectively. These results are in good agreement with previously reported spectra of the $Cr(CO)_5(L)$ complexes.[1-5] No change in band shape or band position is observed for several nanoseconds after photolysis. The transient absorption spectra of longer chain alcohols are found to be similar to that observed in MeOH. However, with increasing chain length, the spectral shape is found to change in time. Depending on the alcohol, from 50 ps to several nanoseconds, the red edge of the absorption band decreases, resulting in a narrowing of the absorption spectrum. As previously discussed, these spectra can be shown to be convolutions of the absorption spectra of alkane- and hydroxyl-coordinated intermediates.[1b,c,3c] The intensity of the transient absorption signal is found to be insensitive to the solvent. Under the assumption that the quantum yield for photodissociation is independent of solvent, this result suggests that the extinction coefficients at the maximum wavelength for the solvated complexes, $Cr(CO)_5L$, are identical within experimental error, ±10%.

In Figure 3, we present the time-dependent transient absorption signal at 520 nm following the photolysis of $Cr(CO)_6$ in neat cyclohexane. $Cr(CO)_6$ does not absorb at 520 nm; absorption at this wavelength reflects the time-dependent populations of the $Cr(CO)_5$(alkane) complex (see Figure 2). The transient signal

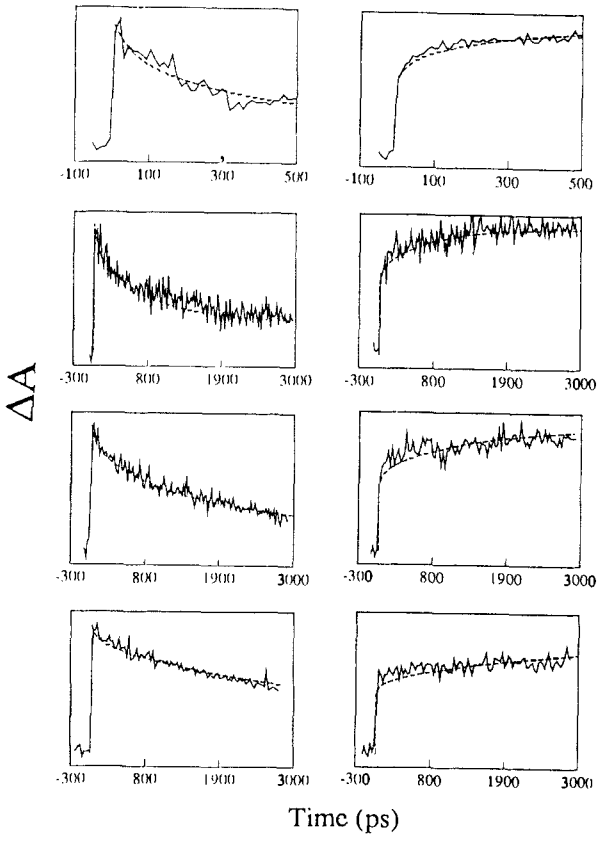

Figure 4. Transient absorption at 520 (left) and 460 nm (right) following photolysis of $Cr(CO)_6$ in alcohol solutions. From top to bottom the solvents are propanol, butanol, pentanol, and octanol. The solid curves are the experimental data. The dashed lines are the fit of the unimolecular kinetic model using initial conditions of random coordination (see text). The maximum transient absorption signals, ΔA, are between 0.02 and 0.04.

rises within the instrument response and exhibits a constant absorption for up to at least 3 ns following photolysis. These data indicate that dissociation is extremely rapid and that coordination of cyclohexane to the metal site occurs within a picosecond.

In alcohol solutions, initial photolysis results in the creating of a distribution of alkane- and hydroxyl-coordinated complexes.[1b] In previous studies, we have examined the transient absorption at 520 and 460 nm in order to determine the time-dependent populations of these species, respectively. We choose 520 nm instead of the maximum of the $Cr(CO)_5$(alkane) complex (500 nm) as there is still significant absorption of the alkane complex at this wavelength but the overlap with the absorption band of the hydroxyl complex is greatly reduced (see Figure 2). In Figure 4, we present the time-resolved absorption signals for the photolysis of $Cr(CO)_6$ in propanol, butanol, pentanol, and octanol at 520 and 460 nm.

For all the alcohol solvents studied, there is an initial instrument-limited rise in the absorption at 460 nm. This is followed by a slow increase in absorption with increasing delay time. The rate of growth of the transient signal is solvent dependent; slower rises are observed with increasing chain length. At 520 nm, an instrument-limited rise is also observed. This is followed by a decrease in absorption with increasing delay time until the signal reaches a constant value. The rate of decrease is also solvent dependent; a slower rate is observed with increasing chain length.

In order to study the effect of solvent structure on the transient absorption dynamics, we examined the photolysis of $Cr(CO)_6$ in 2-Pro. In Figure 5, the data obtained probing at 520 nm are presented. The related studies using ethanol and 1-Pro solutions are plotted for comparison. The decrease in absorption at 520 nm in 2-propanol is more rapid than in 1-propanol but similar to that observed in ethanol. Similar results were observed probing at 460 nm (data not shown).

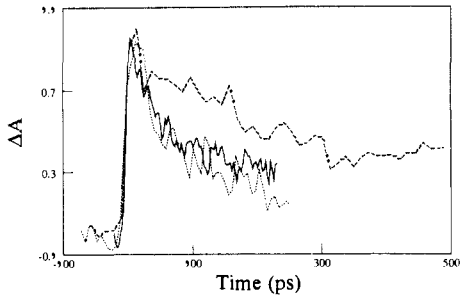

Figure 5. Transient absorption at 520 nm following photolysis of $Cr(CO)_6$ in 1-propanol (---), 2-propanol (···), and ethanol (—). The decay in absorption signal is faster in 2-Pro than 1-Pro, with the dynamics in 2-Pro being similar to that observed in neat ethanol solutions. The three curves are normalized to $\Delta A = 1.0$ for comparison.

Discussion

Photolysis of $Cr(CO)_6$ in solution results in rapid breakage of a chromium–CO bond. The time-resolved data recorded in neat alkane solvent (Figure 3) indicate that bond breakage and solvent coordination occur within a few picoseconds. The nature of the resulting chromium–alkane bond has been the subject of several recent studies. Photoacoustic measurements by Yang et al. reveal a 9.8 kcal/mol bond strength.[3a] This value of the Cr–alkane bond strength is consistent with the idea that shifts in the optical spectra are indicative of increasing bond strength. Comparison of the optical absorption spectra in neon and methane matrices reveals a spectral shift of 12.6 kcal/mol,[7] similar to the experimentally determined bond strength.

As already mentioned, photolysis of $Cr(CO)_6$ in alcohol solutions is known to give rise to a distribution of alkane- and hydroxyl-coordinated complexes.[1b] The data in Figure 4 reflect the time-dependent populations of these complexes. For delay times where the absorption intensities at 460 and 520 nm are constant, there is no transient signal in the region of the absorption band of the alkane complex which is not overlapped by the absorption spectra of $Cr(CO)_5(HOR)$. Thus, the time-independent absorption intensities observed at long delay times reflect only hydroxyl-coordinated intermediates. In this case, the time-dependent changes in the absorption signals at 520 and 460 nm reflect the formation of hydroxyl-coordinated complexes from the initially formed alkane species. Three possible mechanisms for this rearrangement process can be envisioned:[11] dissociation followed by coordination of the hydroxyl group of the same or different solvent molecule, associative substitution, and unimolecular migration between different solvent binding sites. In the following paragraphs, each of these mechanisms is considered in detail and compared to the experimental data.

Dissociative Mechanism. Several reactions of $Cr(CO)_5L$ proceed by dissociative ligand loss. One could then imagine that the restructuring of initially formed alkane complexes to the more stable hydroxyl-coordinated species occurs by such a mechanism. In this case, the decreased rate observed with increasing chain length reflects the fact that following solvent dissociation, the probability of recombining with another alkane group, rather than a hydroxyl group, increases. In a previous report from our laboratory,[1c] transient absorption data for the formation of $Cr(CO)_5(HOR)$ from photogenerated $Cr(CO)_5(ROH)$ in pentanol was explained by using a dissociative mechanism. To account for the experimental data, a dissociation rate in excess of 2×10^9 was invoked. However, the validity of such a model can be tested by considering the dynamics in ethanol and propanol where the effective concentrations of alkane and hydroxyl groups are similar. In this case, the minimum activation energy for the dissociation of the alkane ligand is the metal–ligand bond strength, ≈10 kcal/mol.[3a] We know from the photolysis studies that the rate of solvent association is extremely rapid, $k \geq 10^{-12}$. Thus, the rate-limiting step is expected to be ligand dissociation. Assuming a preexponential factor of 10^{13}[12] and an activation energy of 10 kcal/mol, one calculates a dissociation rate on the order of 4×10^5. The evolution of alkane complexes to the more stable hydroxyl species should occur on the microsecond time scale. The data in Figure 4 suggest rate constants on the order of 10^{10} in ethanol and propanol, 4–5 orders of magnitude faster than that predicted by a dissociative model.

The above discussion relies on an accurate determination of the metal–alkane bond strength. In determining the bond strength by photoacoustics, Yang et al.[3a] assumed a quantum yield for photodissociation of 0.67.[8] In order to account for the dynamics observed in ethanol by a dissociative mechanism, a dissociation rate in excess of 2×10^{10} is needed. Assuming a preexponential factor of 10^{13}, this requires an activation barrier (and hence a maximum Cr–alkane bond strength) of 3.6 kcal/mol. This value is well outside the error bars of the photoacoustic measurements. Thus, a purely dissociative mechanism is not consistent with the experimental data.

Associative Substitution. A second possible mechanism involves associative substitution. This, in effect, would lower the barrier to reaction and result in faster rates than those expected for a dissociative process. There is some evidence to support this model. Yang et al.[3a] measured activation parameters for the thermal substitution reaction

$$Cr(CO)_5(alkane) + L \rightarrow Cr(CO)_5L \qquad (2)$$

where L = pyridine and picoline (2-methylpyridine). They found activation enthalpies of 5.1 and 7.3 kcal/mol for pyridine and picoline, respectively. Both activation barriers are smaller than the metal–alkane bond strength. With increasing steric interactions, the activation energy increased; the rate of substitution of the more sterically hindered picoline was slower than that of pyridine. These two observations are consistent with an associative substitution reaction.

In order to examine whether or not the formation of $Cr(CO)_5(HOR)$ from photogenerated $Cr(CO)_5(ROH)$ is occurring by an associative mechanism, we examined the rearrangement dynamics of 2-propanol and 1-propanol.[1c] The macroscopic properties, i.e., viscosity[13] and Debye relaxation time,[14] of these two solvents are very similar. However, if the reaction is proceeding by an associative mechanism, as observed by Yang et al., one would expect, based on steric considerations, to observe a slower rate in 2-Pro than in 1-Pro. In Figure 5, the transient absorption signal at 520 nm is plotted for the photolysis of $Cr(CO)_6$ in 2-Pro, 1-Pro, and ethanol solutions. The time-dependent signal reflects the disappearance of the alkane-bonded complexes and thus is a direct measure of the reaction dynamics. The dynamics reveal that the reaction occurs faster in the more sterically hindered solvent, opposite to the predictions of an associative substitution reaction. However, the dynamics observed in 2-Pro are very similar to those observed in neat ethanol solution. The similarity between the dynamics observed in ethanol and 2-Pro originally led to the suggestion that the rearrangement of the initially formed alkane complexes is occurring by a unimolecular mechanism.[1c] We now examine such a mechanism in detail and test its applicability to the dynamics observed in longer chain alcohol solvents.

A Unimolecular Solvent Migration Model. (1) The Kinetic Model. In modeling the unimolecular rearrangement process, two rate constants are used, k_{C-C} and k_{C-O}, corresponding to the rate constants for migration between two adjacent alkane groups and an alkane to an adjacent hydroxyl group, respectively. The rate constant k_{C-C} is assumed to be constant for migration between any two adjacent alkane groups. The alkane–metal bond involves electron donation by a C–H bond of the ligand. However, the

(11) (a) For a general discussion of dissociative and associative reaction of metal carbonyl complexes, see: Geoffroy, G. L.; Wrighton, M. S. *Organometallic Photochemistry*; Academic: New York, 1979. (b) Wrighton, M. *Chem. Rev.* **1974**, *74*, 401. (c) Wrighton, M. *Top. Curr. Chem.* **1976**, *65*, 37.

(12) Weston, R. E., Jr.; Schwarz, H. A. *Chemical Kinetics*; Prentice-Hall: Englewood Cliffs, NJ, 1972.

(13) Weast, R. C., Ed. *CRC Handbook of Chemistry and Physics*; CRC Press: Boca Raton, FL, 1983.

(14) (a) Garg, S. K.; Smyth, C. P. *J. Phys. Chem.* **1965**, *69*, 1294. (b) Rizk, H. A. Elanwar, I. M. Z. *Phys. Chem. (Munich)* **1968**, *62*, 225.

kinetic model does not take into account migration between different C–H bonds on the same carbon, nor the fact that the terminal carbon contains one more C–H bond than the middle carbon atoms. Kinetically, this assumption is identical with stating that migration between different sites on a single carbon is much faster than migration between carbon atoms. In addition, we assume that when the metal coordinates to an OH group, no further migration occurs; i.e., the hydroxyl group is considered to be a trap. This assumption is consistent with both the expected difference between the metal–alkane and metal–hydroxyl bond strengths and the lack of transient absorption in the regions of the alkane complex absorption band (not overlapped with the hydroxyl complex band) for long delay times.

The migration kinetics for a linear alcohol molecule containing n carbons can then be represented by n coupled differential equations. The numbering of the carbon atoms in the alkane is sequential, with C^1 being bonded to the OH group. In the particular case of butanol, we would have four coupled differential equations.

$$d[C^1]/dt = k_{C\text{-}O}[C^2] \quad (3)$$

$$d[C^2]/dt = -k_{C\text{-}O}[C^2] - k_{C\text{-}C}([C^2] - [C^3]) \quad (4)$$

$$d[C^3]/dt = k_{C\text{-}C}([C^4] + [C^2] - 2[C^3]) \quad (5)$$

$$d[C^4]/dt = k_{C\text{-}C}([C^3] - [C^4]) \quad (6)$$

In interpreting the meaning of $[C^i]$, we assume the chromium metal to be bonded to the most stable substituent of the reference carbon atom. Thus, the population $[C^1]$ represents the population of hydroxyl-coordinated species. Given a set of initial conditions that describes the distribution of complexes formed immediately following photolysis, the series of coupled differential equations can be simultaneously solved by using the Runge–Kutta algorithm.[15] The solution provides the time-dependent populations of various types of solvent-coordinated complexes. From these data, one would like to calculate the time dependence of the transient absorption signals at the various wavelengths that are probed experimentally. These calculations are carried out as follows.

First, the absorption properties of all alkane complexes are assumed to be identical. Thus, the extinction coefficient and band shape of the optical transient are assumed to be independent of the particular alkane group coordinated to the metal. This assumption is consistent with the observation that the absorption spectrum of the transient intermediate is insensitive to changes in the structure of a neat alkane solvent. Furthermore, there is good agreement between the band shape and band position in methane matrices and alkane solutions.[1,5,7]

Using this approximation, one can calculate the transient absorption by

$$A^\lambda(t) = \epsilon^\lambda_{OH}[Cr(CO)_5(HOR)] + \epsilon^\lambda_{CH}[Cr(CO)_5(ROH)] \quad (7)$$

where ϵ^λ_{OH} and ϵ^λ_{CH} are the extinction coefficients of the hydroxyl and alkane complexes at the wavelength (λ) of interest and $[Cr(CO)_5(HOR)]$ and $[Cr(CO)_5(ROH)]$ are the respective populations of the hydroxyl- and alkane-coordinated complexes. With the notation introduced in the kinetic model, $[Cr(CO)_5(HOR)] = [C^1]$ and

$$[Cr(CO)_5(ROH)] = \sum_{i=2}^{n} C^i \quad (8)$$

where n is the alkane chain length. Since the total number of complexes is independent of time, eq 7 is subject to the constraint $[Cr(CO)_5(HOR)] + [Cr(CO)_5(ROH)] = \text{constant}$.[16] To calculate the absorption signals, one needs the relative extinction coefficients of the hydroxyl and alkane complexes at the various experimental wavelengths studied. These can be determined from the spectra shown in Figure 2. These spectra, collected under identical conditions, provide the needed information as long as one assumes that the quantum yield for photodissociation is independent of solvent. Under these conditions, one obtains $\epsilon^{460}_{OH}:\epsilon^{460}_{CH} = 1.5:1$ and $\epsilon^{520}_{OH}:\epsilon^{520}_{CH} = 1:5$. These relative extinction coefficients are used in the following calculations. If the quantum yield for dissociation were solvent dependent, the above values would lead to errors in the calculations of the time-dependent populations of the alkane- and hydroxyl-coordinated complexes. The effect of varying the $\epsilon_{OH}:\epsilon_{CH}$ ratio on the calculated curves is discussed later.

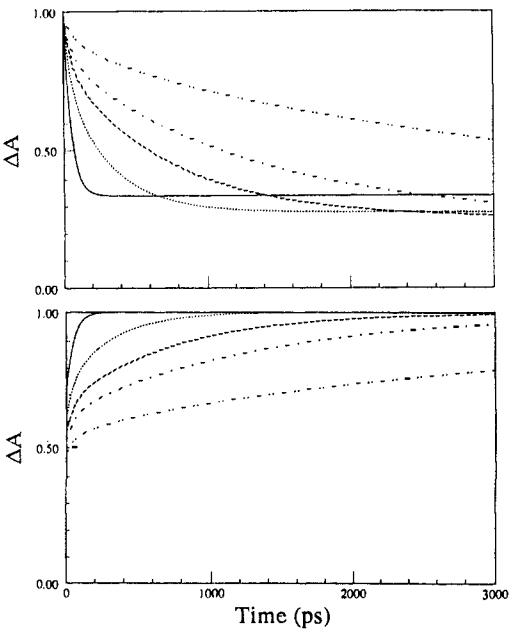

Figure 6. Simulated transient absorption data are plotted for the probe wavelengths 520 (top) and 460 nm (bottom) using the random solvent coordination model (eq 9). Values of 2×10^{10} and 4×10^9 s^{-1} were used for $k_{C\text{-}O}$ and $k_{C\text{-}C}$, respectively. The solvents plotted are (—) ethanol, (···) 1-propanol, (- - -) butanol, (-·-) pentanol, and (-···) octanol.

(2) Calculated Kinetics for Different Initial Conditions. The solution to the set of coupled differential equations depends on the initial populations assigned to the various types of solvent-coordinated complexes. In this section, we examine the predictions of this model by studying two different cases. First, we examine the case where photolysis results in random coordination of the chromium metal to the various solvent sites. This would correspond to the case where the solvent structure around the hexacarbonyl is random and excitation results in photoelimination without consideration of the differences in the local solvent structure around the six carbonyl ligands. This corresponds to an initial condition

$$[C^1](0) = [C^2](0) = \ldots = [C^n](0) = 1 \quad (9)$$

Since the hydroxyl complex is more stable than the alkane species, one would expect a lower activation barrier for the migration between adjacent alkane and hydroxyl groups than for two adjacent alkane moieties, resulting in $k_{C\text{-}O} > k_{C\text{-}C}$. A set of calculated data for the time-dependent absorption signals at 460 and 520 nm, using the initial conditions given in eq 9, are shown in Figure 6. The data were calculated assuming rates of $k_{C\text{-}O} = 2 \times 10^{10}$ s^{-1} and $k_{C\text{-}C} = 4 \times 10^9$ s^{-1}. Several general features can

(15) Small changes from a random distribution, i.e., ±10–20% variation in initial populations between the various solvent sites, also result in excellent fits to the data.

(16) James, M. L.; Smith, G. M.; Woldord, J. C. *Applied Numerical Methods for Digital Computation with Fortran*; International Textbook Co.: Scranton, 1967.

(17) This constraint requires that there is no geminate recombination on the time scale of the rearrangement process. Studies of the photolysis of $Cr(CO)_6$ in weakly bonding solvents, e.g., alkanes[1a,3c] and perfluorinated hydrocarbons,[5] reveal no geminate recombination between a few picoseconds and several nanoseconds. Femtosecond studies[2] also do not reveal any geminate recombination.

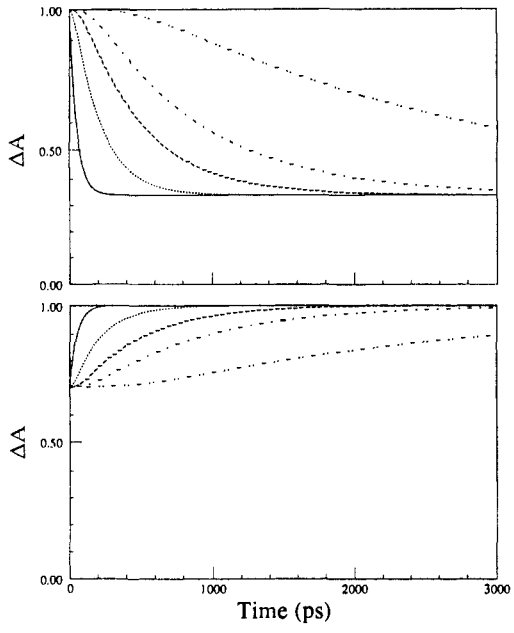

Figure 7. Simulated transient absorption data are plotted for the probe wavelengths 520 (top) and 460 nm (bottom) using the initial conditions that photolysis results in bonding between the metal complex and the terminal ends of the solvent molecule (eq 10 and 11). Values of 2×10^{10} and 8×10^9 s^{-1} were used for k_{C-O} and k_{C-C}, respectively. The solvents plotted are (—) ethanol, (···) 1-propanol, (- - -) butanol, (-··) pentanol, and (-···) octanol.

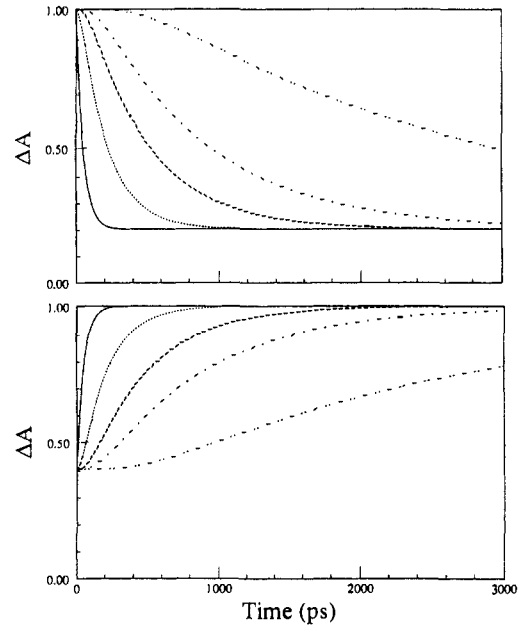

Figure 8. Simulated transient absorption data are plotted for the probe wavelengths 520 (top) and 460 nm (bottom) using the initial condition that the primary intermediate involves exclusive coordination to the terminal alkane group. Values of 2×10^{10} and 8×10^9 s^{-1} were used for k_{C-O} and k_{C-C}, respectively. The solvents plotted are (—) ethanol, (···) 1-propanol, (- - -) butanol, (-··) pentanol, and (-···) octanol.

be seen from the simulated data. First of all, the time-dependent signals are not exponential. Examining the calculated data for 520 nm, we see that the decay curves are concave (to be compared with the terminal-bonded model). If we normalize the calculated curves to 1.0, we find that the final time-independent adsorption value reached is dependent on the alcohol chain length. Decreased absorption values are observed for increasing chain length. This is consistent with the above initial conditions as with increasing chain length, a greater percentage of the initially formed complexes involve coordination to an alkane group. Similarly at 460 nm, if we normalize the final signals to 1.0, the magnitude of the initial pulse limited rise in absorption is chain length dependent, and larger signals are observed with decreasing chain length.

These calculations can be compared to a case where we model the initial solvent distribution as involving a preference to coordination to terminal solvent sites. This could correspond to the case where the solvation of $Cr(CO)_6$ involves the terminal ends of the solvent molecules, as in a "micellar" type structure. If we assume that photolysis resulted in an equal distribution of complexes bonded to the two ends of the solvent molecules, we would have initial conditions of

$$[C^1](0) = [C^n](0) = 1 \tag{10}$$

and

$$[C^2](0) = \ldots = [C^{n-1}](0) = 0 \tag{11}$$

In Figure 7, simulated data using these assumptions are given. If we assumed that $Cr(CO)_6$ was solvated only by the alkane ends of the alcohol molecules, we would have initial conditions of $[C^n] = 1$ and $[C^i] = 0$ for $i < n$. Simulations for this limiting case are shown in Figure 8. The rate constants used for these calculations are 8×10^9 s^{-1} and 2×10^{10} s^{-1} for k_{C-C} and k_{C-O}, respectively. Once again, in both Figures 7 and 8, the absorption dynamics are nonexponential. However, in contrast to the random coordination conditions, for normalized data, the final absorptions observed at 520 nm and the magnitude of the initial absorption rise at 460 nm are independent of alcohol chain length. In addition, for equal bonding to both ends of the solvent molecule, the curvature of the decays at 520 nm is now convex rather than concave. If one assumes initial bonding to only the alkane end of the molecule, the calculated curves exhibit a constant absorption

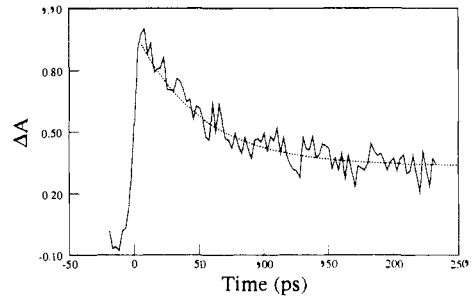

Figure 9. Time-resolved absorption at 520 nm for photolysis of $Cr(CO)_6$ in ethanol. The dashed line is a fit of the unimolecular reaction model, resulting in a rate constant for migration between the alkane and hydroxyl group, k_{C-O}, of 2×10 s^{-1}. The data are normalized to $\Delta A = 1.0$ to facilitate comparison with calculations.

for a period of time following photolysis, followed by a decay in absorption at 520 nm which also exhibits convex curvature.

The exact dynamics calculated are dependent on the initial conditions chosen. Cases between those considered here give results that are between those depicted in Figures 6–8.

(3) Fitting the Experimental Data. In addition to a set of initial conditions, the rate constants k_{C-C} and k_{C-O} need to be determined in order to model the experimental data. k_{C-O} can be determined directly from the time-resolved data obtained in ethanol. In this solvent, only a one-step migration process is possible. Simultaneous fitting of the data at 460 and 520 nm suggests that (1) $k_{C-O} = 2 \pm 0.2 \times 10^{10}$ s^{-1} and (2) photolysis results in approximately equal amounts of alkane and hydroxyl complexes. The fit to the data for 520 nm is shown in Figure 9. In light of the above discussion, these results suggest that coordination of $Cr(CO)_5$ to ethanol is occurring randomly. It is reasonable to assume that k_{C-O} will be independent of chain length. As a result, we will use this value for all the alcohols studied. The value of k_{C-C} is more difficult to determine. However, on the basis of the relative stability of the alkane and hydroxyl complexes, one expects $k_{C-C} < k_{C-O}$. One approach is to assume a set of initial conditions and then try to fit the entire set of experimental data by using a single value for k_{C-C}.

Before carrying out comparisons between calculated and experimental curves, one can obtain insight into the appropriate

choice of initial conditions by examining the data in Figure 4 and comparing the behavior exhibited by the various limiting cases given in Figures 6-8. First, no delay in the decay in the transient absorption signal at 520 nm is observed following photolysis. Thus, models that involve preferential bonding to the terminal alkane region of the solvent will not be able to describe the experimental data. Second, the decay curves exhibit a concave rather than convex curvature. Thus, models that only involve binding to the ends of the solvent will also fail in describing the data. These observations along with the distribution extracted from the ethanol data suggest that a random (or nearly random) solvent coordination model is appropriate.

In Figure 4, the dashed lines are the best fit of a random bonding model (eq 9) requiring that a single rate constant for k_{C-C} be used to fit the entire set of data. The best value found for k_{C-C} was 4×10^9 s^{-1}. The agreement between the calculated and experimental curves for the entire set of data using this rate constant for the migration between carbon atoms strongly supports the conclusion that a unimolecular reaction model can account for the transient absorption dynamics.

We attempted to fit the data using other sets of initial conditions. Small changes from a random distribution have essentially no effect on the quality of the fit. However, as described qualitatively above, models that bias the terminal regions or the center regions of the chain show poor agreement with the data. These observations strongly suggest that photolysis results in random coordination of the metal to all available solvent sites.[15]

In carrying out these simulations, we assumed that the quantum yield for dissociation was solvent independent, thus allowing one to determine relative values of ϵ_{OH} and ϵ_{CH} directly from transient absorption measurements. If this assumption is not true, then from eq 7, the simulated curves would be affected. We have examined the effect of the ϵ_{OH}:ϵ_{CH} ratio on the calculated curves. Changes in this ratio by ±20% had only a small effect on the determination of either k_{C-O} or k_{C-C}. In any case, the agreement between the calculated and experimental data is similar to that shown in Figure 4.

In these calculations we have not taken into account the potential role of hydrogen bonding between alcohol molecules. It is possible that in the $Cr(CO)_5(ROH)$ complex the hydroxyl end of the coordinated molecule is hydrogen bonded to a second solvent molecule. In this case, formation of $Cr(CO)_5(HOR)$ would not only involve rupturing of a Cr-alkane bond but also an intermolecular hydrogen bond. Insight into the time scales for this latter process can be obtained from dielectric relaxation studies. The longest Debye relaxation time observed for neat alcohol solutions is commonly associated with the dynamics of intermolecular hydrogen bond breakage.[14a] At 20 °C the Debye relaxation time ranges from 196 ps for ethanol to 1.2 ns for hexanol. These relaxation times are significantly longer than those reflected by the time-resolved absorption data for the relaxation of photogenerated $Cr(CO)_5(ROH)$ to $Cr(CO)_5(HOR)$. From this comparison, we conclude that the rate of breakage of an intermolecular hydrogen bond does not affect the kinetics of the migration process.

Acknowledgment. This work is supported by the National Science Foundation. J.D.S. thanks Professor Peter Armentrout for his suggestion of the unimolecular reaction model. We thank Professor Keith Nelson for preprints of his femtosecond work.

Registry No. $Cr(CO)_6$, 13007-92-6; *i*-Pro, 67-63-0; cyclohexane, 110-82-7; methanol, 67-56-1; ethanol, 64-17-5; *n*-propanol, 71-23-8; butanol, 71-36-3; pentanol, 71-41-0; octanol, 111-87-5.

Heteroatom-Directed π-Facial Diastereoselection in Diels–Alder Cycloadditions of Plane-Nonsymmetric Cyclopentadienes

John B. Macaulay and Alex G. Fallis*

Contribution from The Ottawa-Carleton Chemistry Institute, Department of Chemistry, University of Ottawa, Ottawa, Ontario, Canada K1N 6N5. *Received June 1, 1989*

Abstract: The synthesis of a series of pentamethylcyclopentadienes bearing stereogenic C-5 heteroatom substituents and their reactions in [4 + 2] cycloadditions with maleic anhydride and/or *N*-phenylmaleimide are described. Cyclopentadienes (**13**, **14**, **6**, **7**, and **1**) containing the substituents OH, OCH_3, NH_2, NHAc, and Cl reacted to form syn adducts preferentially. In contrast, with compound **8** (SH) only slight syn discrimination was observed, while the facial selectivity was reversed with other sulfur substituents (SCH_3, SPh, SCH_2Ph, $SOCH_3$, SO_2CH_3) (compounds **9**, **3**, **2**, **10**, and **11**), and anti adducts were the major or exclusive products. This behavior is consistent with the σ donor ability of the C–X versus the C–C bond so that cycloaddition occurs preferentially anti to the best donor due to hyperconjugation of this antiperiplanar σ bond with the developing incipient bond(s).

The synthetic utility of the Diels–Alder reaction is well-established.[1] Its continued popularity and study rests, in part, on the ability to generate four new contiguous stereogenic centers in one synthetic step. The regiochemistry may be controlled by the appropriate choice of substituents, and the topography (endo or exo) may be influenced by the electronic nature of the groups attached to the dienophile. A third stereochemical feature, the π-facial diastereoselectivity, which arises when the addends possess two different reactive faces is also important. Frequently the presence of at least one center of chirality imparts sufficient perturbation to influence the diastereofacial selectivity. Alternatively, facial selectivity can be influenced by a chiral auxiliary in which one face of the diene or dienophile is blocked preferentially.[2] Incorporation of a single stereogenic center in an allylic position of either a dienophile or a diene, particularly when a heteroatom is present, is known to exert a directing influence, although the exact factors responsible for the observed facial stereoselection are still imperfectly understood. Nevertheless,

(1) (a) Desimoni, G.; Tacconi, G.; Bario, A.; Pollini, G. P. *Natural Product Syntheses through Pericyclic Reactions*; ACS Monograph 180; American Chemicalla Society: Washington, DC, 1984; Chapter 5.

(2) (a) Helmchen, G.; Karge, R.; Weetman, J. *Modern Synthetic Methods*; Scheffold, R., Ed.; Springer Verlag: New York, 1986; p 261. (b) Paquette, L. A. *Asymmetric Synthesis*; Morrison, J. D., Ed.; Academic Press: New York, 1984; Chapter 7. (c) Oppolzer, W. *Angew. Chem., Int. Ed. Engl.* **1984**, 876.

0002-7863/90/1512-1136$02.50/0